Heliyon 8 (2022) e12126

Contents lists available at ScienceDirect

Heliyon

journal homepage: www.cell.com/heliyon

Research article

An integrative exploration of loquat leaf total sesquiterpene glycosides in treating insulin-resistant mice by serum and urine untargeted metabolomics analysis

Yanan Gai [a], Jiawei Li [a], Tunyu Jian [a], Xiaoqin Ding [a], Han Lyu [a], Yan Liu [a], Jing Li [b], Bingru Ren [a], Jian Chen [a,b,*], Weilin Li [a,b]

[a] Institute of Botany, Jiangsu Province and Chinese Academy of Sciences, Nanjing 210014, China
[b] Department of Food Science and Technology, College of Light Industry and Food Engineering, Nanjing Forestry University, Nanjing 210037, China

GRAPHICAL ABSTRACT

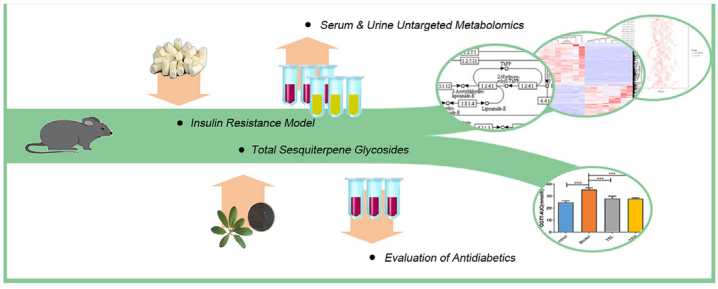

ARTICLE INFO

Keywords:
Total sesquiterpene glycosides
Insulin resistance
Untargeted metabolomics
Lipid metabolism
Metabolic pathway
Loquat leaf

ABSTRACT

Loquat leaf is approved to be beneficial in the treatment of diabetes. Total sesquiterpene glycosides (TSG), a major chemical component cluster, has potential ability to improve insulin-resistant diabetes syndrome. Its therapeutic mechanism using metabolomics *in vivo* is worth to be investigated. This study aimed to reveal the underlying therapeutic mechanism of TSG on insulin-resistant mice by untargeted metabolomics, and to explore the lipid metabolism differences *in vivo*. High-fat diet was used to induce insulin-resistant mice model. Biochemical indicators were applied to evaluate the model validity and related treatment effect. Ultra-performance liquid chromatography quadrupole-time-of-flight mass spectrometry was utilized to accomplish serum and urine untargeted metabolomics. Oral administration of TSG had a therapeutic effect on high-fat diet induced insulin-resistant mice. Four hundred forty-two metabolites in serum and 1732 metabolites in urine were annotated. Principal component analysis screened 324 differential metabolic signatures in serum sample and 1408 in urine sample. The pathway mainly involved purine metabolism and biosynthesis of unsaturated fatty acids. Lipidomic analysis of urine and serum confirmed that most lipid metabolites were fatty acyls, sterol lipids and polyketides.

* Corresponding author.
E-mail address: chenjian80@aliyun.com (J. Chen).

https://doi.org/10.1016/j.heliyon.2022.e12126
Received 10 May 2022; Received in revised form 26 October 2022; Accepted 28 November 2022

1. Introduction

Loquat leaf, the leaves of *Eriobotrya japonica* (Thunb.) Lindl., has been approved to possess multiple bioactivities such as anti-inflammatory, anti-diabetes, anti-cancer and antioxidant [1]. The observed chemical components of loquat leaf were flavonoids [2, 3], organic acids [4], triterpene acids [5], sesquiterpenes and other micromolecule compounds. Sesquiterpene glycosides, an essential class of effective ingredients in loquat leaf, can be mainly divided into chain, single cyclic and ionone sesquiterpene glycosides (Figure 1 presents their chemical frame structures) according to the structure of aglycone [6, 7, 8, 9, 10, 11]. Some of the chain sesquiterpenoid glycosides were approved to be pharmacological active substances (substituent type of 4 compounds were named in footnote). Compared with compound 1 and 2, compound 3 had a significant hypoglycemic effect in C57BL/KsJ-db/db/Ola genetic diabetes mice model. Chen et al. [12] had verified that compound 2 could reduce the blood glucose level of type 1 diabetic mice induced by alloxan. In addition, compound 4 was approved to be a histothrombin inhibitor, with potential antithrombotic activity. Currently, studies have tested the efficacy of total sesquiterpenoid glycosides (TSG), which includes such active constituents. It is now well established that TSG was effective in improving lipid accumulation against Nonalcoholic fatty liver disease (NAFLD) *in vitro* and *in vivo* [13]. In HepG2 cells of NAFLD induced by oleic acid, TSG was found to reduce lipid deposition. It could also decrease total triglyceride (TG), cholesterol (TC) and intracellular free fatty acid (FFA) contents probably by downregulating CYP2E1 expression and JNK/c-Jun phosphorylation. Furthermore, TSG ameliorated high-fat diet induced excessive fat accumulation in the NAFLD mice [14, 15]. Generally, TSG is effective and has potential scope in the improvement of insulin-resistant diabetes syndrome. However, the therapeutic mechanism and metabolism situation of TSG therapy remain unrevealed.

Diabetes mellitus (DM) is a metabolic disease characterized by hyperglycemia induced by genetic and environments factors. As a common metabolic disease, DM is mainly caused by insulin resistance (type 2 diabetes mellitus, T2DM) and insulin secretion dysfunction (type 1 diabetes mellitus, T1DM). Except for gestational and special types of diabetes, most DM patients are affected by T2DM, mainly caused by defects with relatively insufficient insulin production or blocked receptors [16]. DM is also usually associated with different degrees of sugar, protein and lipid metabolic disorders [17, 18].

Lipometabolic disturbance (LD), one of the most common pathophysiological changes in the development of T2DM, is an important risk factor leading to complications such as atherosclerosis, cerebrovascular and coronary heart disease. This kind of lipid abnormality in blood, tissues and organs aggravates insulin resistance and directly acts on islets to cause apoptosis of β cells, resulting in dysfunction and dysregulation [19]. Existing literature has explored a higher fat accumulation and decomposition rate of visceral adipose tissue than subcutaneous adipose tissue [19]. It may cause insufficient oxygen supply in the tissue and increase secretion of adipocytokines and macrophage infiltration [20, 21]. Clinical studies have shown that fat accumulation in the visceral is an important cause of metabolic diseases such as insulin resistance and T2DM [22]. Therefore, metabolism including lipid metabolism of T2DM and its therapy need to be evaluated urgently.

Metabolomics is an integral and dynamic technological method to study typical chronic metabolic diseases by discovering abnormal metabolic changes caused by diseases at the molecular level. Therefore, it is often applied in studying diabetes. Typically, the complex metabolism involved in diabetes leads to difficulties in the revelation of pathophysiological process and mechanism. Unignorably, the interaction between traditional Chinese medicine (TCM), essentially their chemical components, and human bodies often benefits from its multi-effect and multi-target mode of mechanism. Therefore, metabolomics presents an obvious advantage in studying diabetes treated with complex TCM components. Analyses on the composition and variation of endogenous metabolites in biological samples can explain the physiological and pathological conditions of subjects and reflect the metabolic rules in the overall metabolism affected by TCM [23, 24]. Many metabolites and differential biomarkers related to the pathogenesis of metabolic diseases and TCM treatment have been found through metabolomic studies. TCM therapy may alleviate metabolic disorders by regulating the metabolism of glucose [25], lipid and amino acid [26], reducing lipid peroxidation

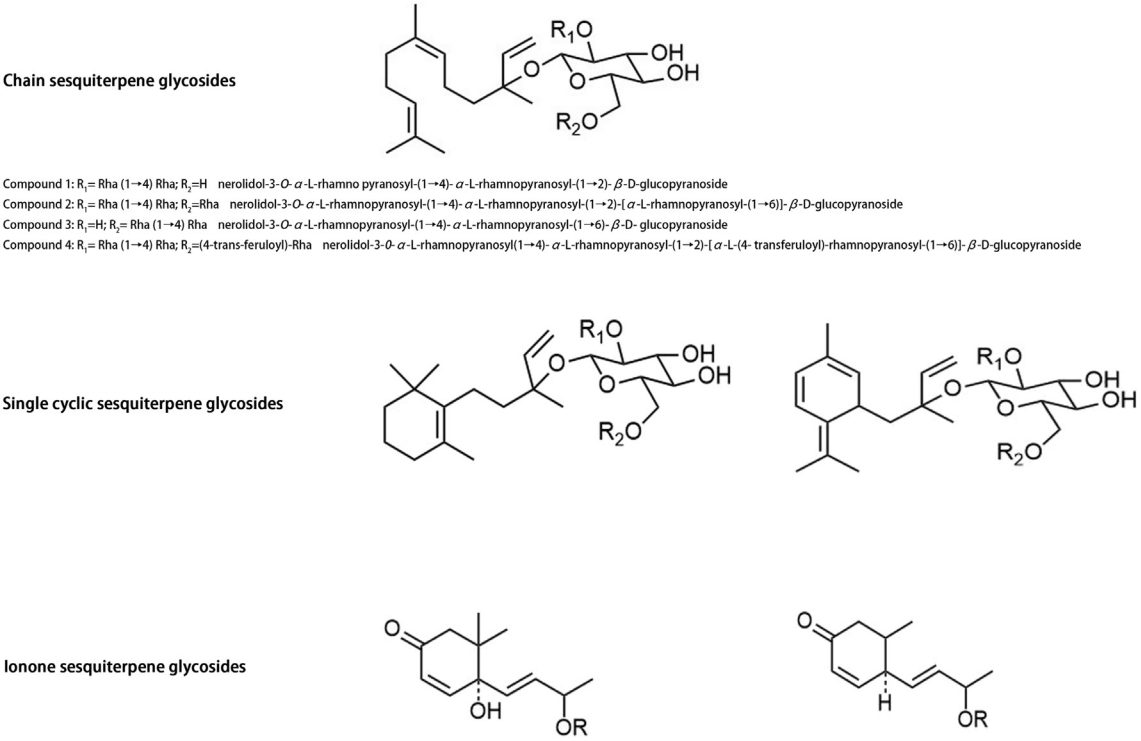

Figure 1. Chemical structures of chain sesquiterpene glycosides, single cyclic sesquiterpene glycosides, and ionone sesquiterpene glycosides.

products [27], improving the body insulin sensitivity [28], and relieving inflammation [29], eventually to be able to ameliorate diabetes [30, 31].

The study aimed to reveal the therapeutic mechanism of TSG on insulin-resistant mice by untargeted metabolomics, sketching the changes of metabolites in blood and urine after TSG therapy, digging in the metabolic perturbation pathways, and identifying key compounds in regulation.

2. Materials and methods

2.1. Materials and chemicals

Loquat leaves were collected from Xishan Island (Suzhou, China) and authenticated as the leaf of *Eriobotrya japonica* (Thunb.) Lindl. by Professor Bing-ru Ren (Institute of Botany, Jiangsu Province and Chinese Academy of Sciences, Nanjing, China). The voucher specimens (No.328636) were deposited in the Herbarium of Institute of Botany, Jiangsu Province and the Chinese Academy of Sciences.

HPLC-grade methanol, formic acid and ammonium acetate were purchased from Thermo Fisher Scientific (Waltham, Massachusetts, USA).

TC, TG, low-density lipoprotein cholesterol (LDL-C), high-density lipoprotein cholesterol (HDL-C), activity assay kits were obtained from Nanjing Jiancheng Bioengineering Institute (Nanjing, China). ELISA Kit for Insulin were obtained from Multisciences Biotech (Hangzhou, China). All the other chemicals and reagents were of analytical grade.

2.2. Preparation of TSG

TSG was prepared according to our previous experiment [16]. Briefly, 50 kg loquat leaves were dried, crushed and soaked in 80% ethanol (1:8, v/v) at room temperature for 2 months. After a vacuum concentration, the concentrated solution was centrifuged for 15 min with a rotate speed equal to 3000 g, then the supernatant was separately eluted by 0, 40%, 60%, 70%, and 95% EtOH using a column chromatographed equipted with macroporous resin (XAD16). Afterward, fraction of 60% and 70% EtOH were combined, evaporated, and chromatography separated using polyamide as stationary phase, H_2O, MeOH and their mixtures (7:3, 5:5, 3:7) as eluant. The H_2O eluted fraction was collected and eluted with pure MeOH and H_2O–MeOH mixtures (9:1, 7:3, 5:5, 4:6, 3:7, 8:2) on a RP-C18 column. The mixture of 5:5–3:7 fractions were concentrated, and 8.1492 g TSG was finally obtained.

2.3. Animals and insulin resistance (IR) model

Male SPF C57BL/6J mice (certificate No. SCXK2013-0016), weighing 18–22 g, were bought from Sino-British SIPPR/BK Lab Animal Co., Ltd (Shanghai, China). The mice were raised in a laboratory environment room under light-dark cycle (12:12 h) with free access to food and water for acclimatization. At the beginning, the mice got a nine-week treatment as follows [32]: regular diet (certificate No. 201401008, Xietong Organism Inc., Nanjing, China) for the control group, high-fat diet (containing 74% feedstuff as control group, 10% sucrose, 10% lard, 5% egg yolk powder, 1% cholesterol, 0.2% pig bile salt) for the others. Then, high-fat diet fed the animals were randomly divided into three groups, each group contained eight mice: IR model group, high dose therapy group (TSH, 200 mg/kg of TSG) and low dose therapy group (TSL, 100 mg/kg of TSG). All the mice were gavaged once daily with equal volume saline or TSG for another 9 weeks. All the animal experiments in this study obeyed the *Guide for the Care and Use of Laboratory Animals* approved by the Animal Ethics Committee of China Pharmaceutical University (SYXK2016-0011, Jan 27, 2016–Jan 26, 2021).

After treatment, as mentioned in Section 2.4, the mice experienced the oral glucose tolerance test (OGTT) and the insulin tolerance test (ITT) successively during the following week. Then the mice were placed in a metabolic cage. Urine samples were collected during 1 h in the morning. The mice blood was collected from eyes with sodium pentobarbital anesthesia (50 mg/kg I.P.). After centrifuged, the serum and the urine samples were gently drained and stored at -80 °C.

2.4. OGTT and ITT

After an overnight fasting, mice were given intragastric administration of 2 g/kg glucose solution (OGTT) or intraperitoneal injection of 0.8 U/kg insulin. Blood sampling was held at 0, 30, 60, 120, 180 min from the vein of the inner canthus, fasting but free to drink in this period The blood glucose was measured by the glucose dehydrogenase method. OGTT and ITT curves were drawn, and areas under the curve (AUC) were calculated, respectively.

2.5. Biochemical parameters analysis

Serum glucose, TC, TG, HDL-C and LDL-C levels were quantified by microplate reader (Molecular Device, CA, USA). Serum insulin was determined by ELISA commercial kit. All of the operations were carried out following commercial kits instructions.

2.6. Serum and urine sample collection

The whole blood was drawn from the orbit and stored at room temperature for 1 h to solidify and layer. After centrifugation at 3000 rpm for 5 min, the supernatant was transferred and centrifuged again at 12,000 rpm at 4 °C for 10 min. Finally, the supernatant serum was removed to store at -80 °C until use. The urine was collected in the morning during 1 h and quench immediately with liquid nitrogen for 15 min. After centrifuged at 12,000 rpm, the supernatant was removed to Eppendorf tube and filtrated by 0.22 μm filter. The filtrate was stored in a refrigerator at −80 °C for future use. The serum and urine of control group, model group and TSH group were used furtherly in metabolism analysis.

2.7. Sample preparation

Prechilled methanol (400 μL) was added to every 100 μL liquid serum or urine sample to precipitate proteins. Then the liquid samples were dried and resuspended with 400 μL prechilled methanol - water (V:V = 4:1, with 0.1% formic acid in water) by well vertexing. The samples were incubated on ice for 5 min and then centrifuged at 15000 rpm, 4 °C for 10 min. 300 μL of the supernatant was diluted by 100 μL LC-MS grade water to make the sample containing 60% methanol. The samples were subsequently filtrated by an Eppendorf tube with a 0.22 μm filter. Finally, the filtrate was injected into the LC-MS/MS system analysis.

Blank sample was 60% methanol aqueous solution containing 0.1% formic acid instead of experimental sample, and the pretreatment process was the same as experimental sample. Quality control (QC) sample was obtained by mixing equal aliquots (30 μL) from each experimental sample. Before analysis, 6 QC samples were run to balance the system. QC samples were injected at fixed intervals (every 10 samples) during the analysis process.

2.8. UPLC-Q-TOF-MS analysis

Vanquish Horizon UPLC system were used for LC-MS/MS analyses coupled with an Orbitrap Q Exactive HF-X mass spectrometer (Thermo Fisher). Samples were injected and separated by Hyperil Gold column (C18, 100 × 2.1 mm, 1.9μm). Mobile phase for positive ion monitoring mode were eluent A (0.1% FA in Water) and eluent B (Methanol), for negative mode were eluent A (5 mM ammonium acetate, pH 9.0) and eluent B (Methanol). A 16-min linear gradient was used: 0–1.5 min, 2% B; 12.0 min, 100% B; 14.0 min, 100% B. The flow rate was 0.2 mL/min . Mass spectrometric detection was operated in positive and negative polarity mode separately. The spray voltage was set as 3.2 kV, the capillary temperature was set as 320 °C, the sheath gas flow rate and aux gas flow

rate were set as 35 arb and 10 arb. Data of mass spectra were obtained within the mass range of 200–1500 *m/z*.

2.9. Data analysis

All the results in animal experiments were presented as means ± SD (standard deviation). Statistical significance was determined using one-way ANOVA followed by Student's t-tests between groups. P value $\leq$ 0.05 was considered statistically significant. For metabolomics analyses, raw data files were generated by UPLC-MS/MS. Then Compound Discoverer 3.0 (CD 3.0, Thermo Fisher) were used to process peak alignment, peak picking, and quantitation Retention time tolerance was set as 0.2 min; signal intensity tolerance was set as 30%; actual mass tolerance was set as 5ppm; minimum intensity, 100000 and SNR (signal to noise ratio), 3. Subsequently, peak intensities were normalized by relative peak abundance towards QC samples. PCA (Principal component analysis) and PLS-DA (partial least squares discriminant analysis) were performed with MetaboAnalyst. The normalized data were used to predict the Molecular formula were predicted according to fragment ions, additive ions and molecular ion peaks. Then peaks were matched with mzCloud (https://www.mzcloud.org/) and ChemSpider (http://www.chemspider.com/) database. Accurate qualitative and relative quantitative results were obtained.

3. Results

3.1. Effects of TSG on high-fat diet induced IR mice model

As shown in Figure 2A after 9 weeks of high-fat diet, compared with the control group, mice in the model group represented significantly increased body weight ($^{\#\#}P < 0.01$). After a 9-week administration with TSG, at the end of the 18th week, the body weight of both TSL and TSH groups persuaded a deep fall compared with the model group (***P < 0.001). In addition, TC, TG and LDL-C levels (Figure 2B–D) were found decreased (*P < 0.05, ***P < 0.001), while HDL-C levels (Figure 2E) increased (**P < 0.01, ***P < 0.001) in serum compared with the model group.

As shown in Figure 2F and G, compared with control group, the blood glucose level and the area under the curve (AUC) of model group were significantly increased ($^{\#\#\#}P < 0.001$). On the contrary, compared with model group, the levels of blood glucose and AUC of TSL and TSH treatment groups came down apparently (***P < 0.001). It indicated an improved glucose tolerance in TSL and TSH treatment groups. Similarly, as shown in Figure 2H and I, compared with control group, the blood insulin level and the AUC of model group were significantly increased ($^{\#\#\#}P < 0.001$). Compared with model group, the levels of blood insulin and AUC of TSL and TSH treatment groups came down correspondingly (***P < 0.001), indicating a recovery of insulin tolerance in TSL and TSH treatment groups. The findings supported that insulin-resistant mice model was established successfully by nine-week treatment of high-fat diet. It also implied that TSG had a therapeutic effect on high-fat diet induced insulin-resistant mice.

3.2. Characterization of metabolic differences

3.2.1. Data quality control

The system stability was validated by QC sample injection occasionally during the whole sample analysis. The Pearson correlation coefficient between QC samples was calculated based on the peak area value. $R^2 \geq 0.98$ in serum and urine sample under both positive and negative mode. PCA of total samples was done subsequently. The peaks extracted from all experimental samples and QC samples were processed by Pareto-scaling and PCA. QC samples distributed together as cluster. The results of data quality control verified a good stability and high quality of the analytical method. Pearson correlation coefficient and PCA analysis diagram were shown in Supplementary Material 1, data of Pearson correlation coefficient was list in Supplementary Material-Pearson correlation as reference material.

3.2.2. Metabolite function and annotation

According to the relative standard deviation (RSD) of QC samples (RSD < 30%), in the serum, 793 metabolites were identified under the positive ion mode, 872 under the negative ion mode. These numbers were 3241 and 2616 correspondingly in the urine.

Based on KEGG database, by comparing secondary mass spectrometry information, totally 442 metabolites (206 under positive mode, 236 under negative mode) in serum and 1732 metabolites (952 under positive mode, 780 under negative mode) in urine were annotated. The number of metabolites in different function were figured out and shown in Supplementary Material 2 as reference material. It was found that metabolites found in serum and urine were mostly relevant to the function of amino acid metabolism, lipid metabolism, and digestive system (with annotated metabolites >40).

3.2.3. Differential metabolites

In order to reveal the underlying metabolic perturbation, multivariate statistical analysis was performed. PCA showed an obvious separation between the TSG groups and control group, with PC1 at 11.6%, PC2 at 38.76% under the positive ion mode and PC1 at 12.2%, PC2 at 45.88% under the negative ion mode for serum sample; PC1 at 63.60%, PC2 at 10.72% under the positive ion mode and PC1 at 63.15%, PC2 at 14.45% under the negative ion mode for urine sample (Supplementary Material 3A and B). Significant discrimination in metabolic phenotypes was further observed from the PLS-DA mode with the R2Y of 0.99, Q2Y of 0.91, R2 of 0.77, Q2 of −0.82 under the positive ion mode and R2Y of 0.99, Q2Y of 0.96, R2 of 0.66, Q2 of −0.78 under the negative ion mode for the serum; R2Y of 1.00, Q2Y of 1.00, R2 of 0.65, Q2 of −0.82 under the positive ion mode and R2Y of 1.00, Q2Y of 1.00, R2 of 0.49, Q2 of -0.91 under the negative ion mode for the urine (Supplementary Material 3C and D). Variable Importance in the Projection (VIP) value represents the contribution rate of different metabolites in different groups; the threshold was set as VIP > 1.0, the difference multiple Fold Change (FC) > 2.0 or FC < 0.5 and the P value < 0.05. With the comparison of model group and control group, 324 differential metabolic signatures in serum sample and 1408 in urine sample were screened under both positive and negative mode: 136 significantly up-regulated and 188 significantly down-regulated in the serum; 885 significantly up-regulated and 523 significantly down-regulated in the urine. The number of differential metabolites between TSG groups and model group were 300 in serum sample and 466 in urine sample under two ion modes with 145 up-regulated, 155 down-regulated in the serum, 214 up-regulated and 252 down-regulated in the urine (Supplementary Material-Differential metabolites). The volcanic plot visually exhibited the overall distribution of differential metabolites (Figure 3A and B). The abscissa represented the expression changes of metabolites in different groups (log2FC, log base two of Fold Change). The ordinate represented the level of significance difference (−log10 P-value). As shown in Venn diagram, there were 153 urine metabolites and 64 serum metabolites that had been simultaneously regulated in all the three groups (Figure 3C and D).

3.2.4. Metabolic pathway annotation of differential metabolites

Hypergeometric test was applied to KEGG (https://www.genome.jp/kegg) pathway enrichment analysis. Compared with all the identified metabolite backgrounds, pathways of biochemical metabolism and signal transduction which differential metabolites took part in was established. The enrichment KEGG bubble diagram presented the number of differential metabolites in the top 20 pathways and p-value compared TS with Model group in serum (Supplementary Material 4A) and urine (Supplementary Material 4B).

Compared TS with Model group, Purine metabolism, Caffeine metabolism, alpha-Linolenic acid metabolism was significant interfered, with

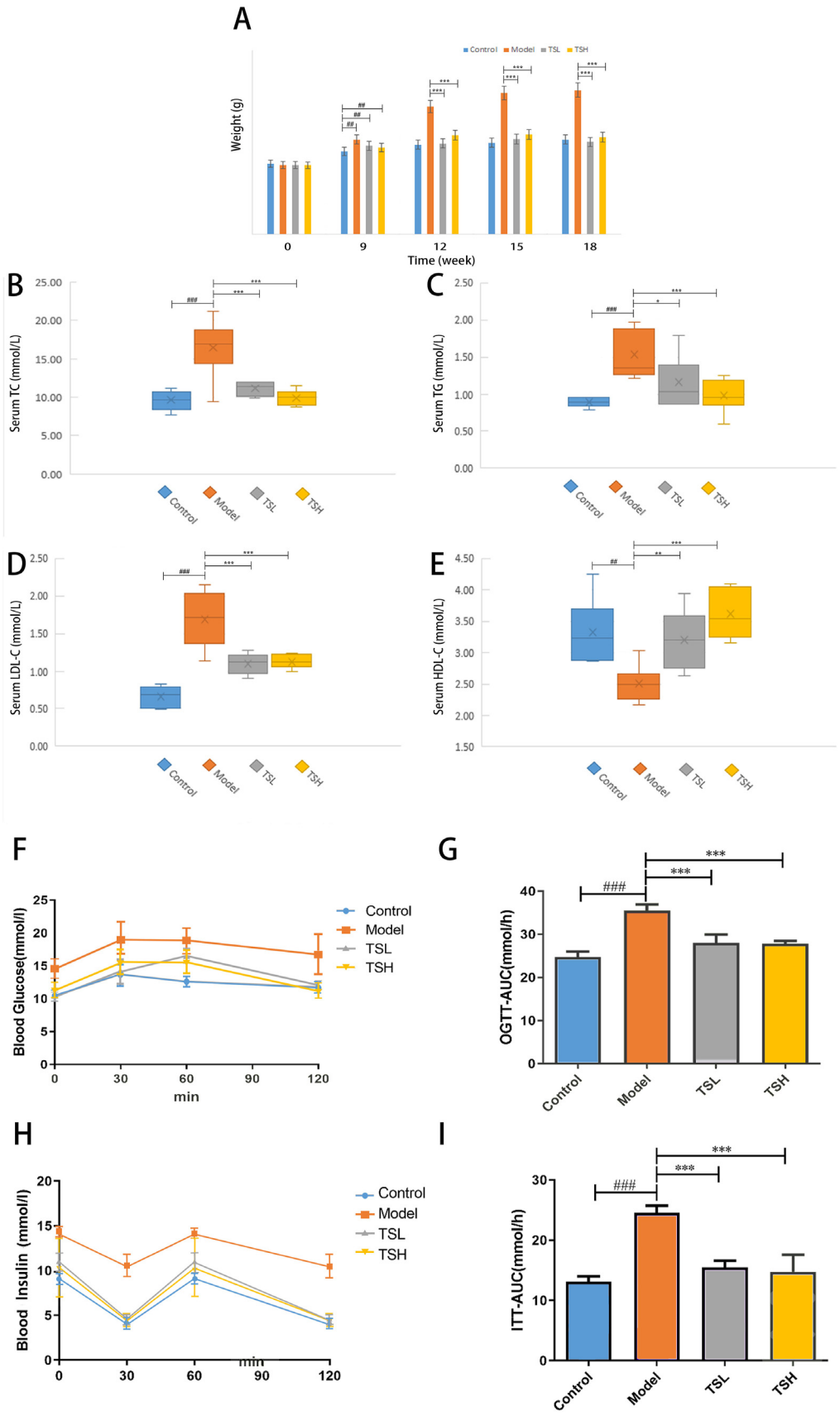

Figure 2. Effects of TSG on diets induced IR mice (A) Body weight of IR mice during 18 weeks. Control (n = 10 mice), Model (n = 10 mice), TSH (100 mg/kg, n = 9 mice) and TSL (25 mg/kg, n = 19 mice). Quantitation of (B) TC, (C) TG, (D) LDL-C and (E) HDL-C. Quantitation of (F) blood glucose, (G) OGTT, (H) blood insulin, and (I) ITT. All data were presented as mean ± SEM. $^{\#\#}P < 0.01$, $^{\#\#\#}P < 0.001$, significant difference compared with Control group. $^{*}P < 0.05$, $^{**}P < 0.01$, $^{***}P < 0.001$, significant difference compared with Model group. Statistical differences between group means were determined by one-way ANOVA.

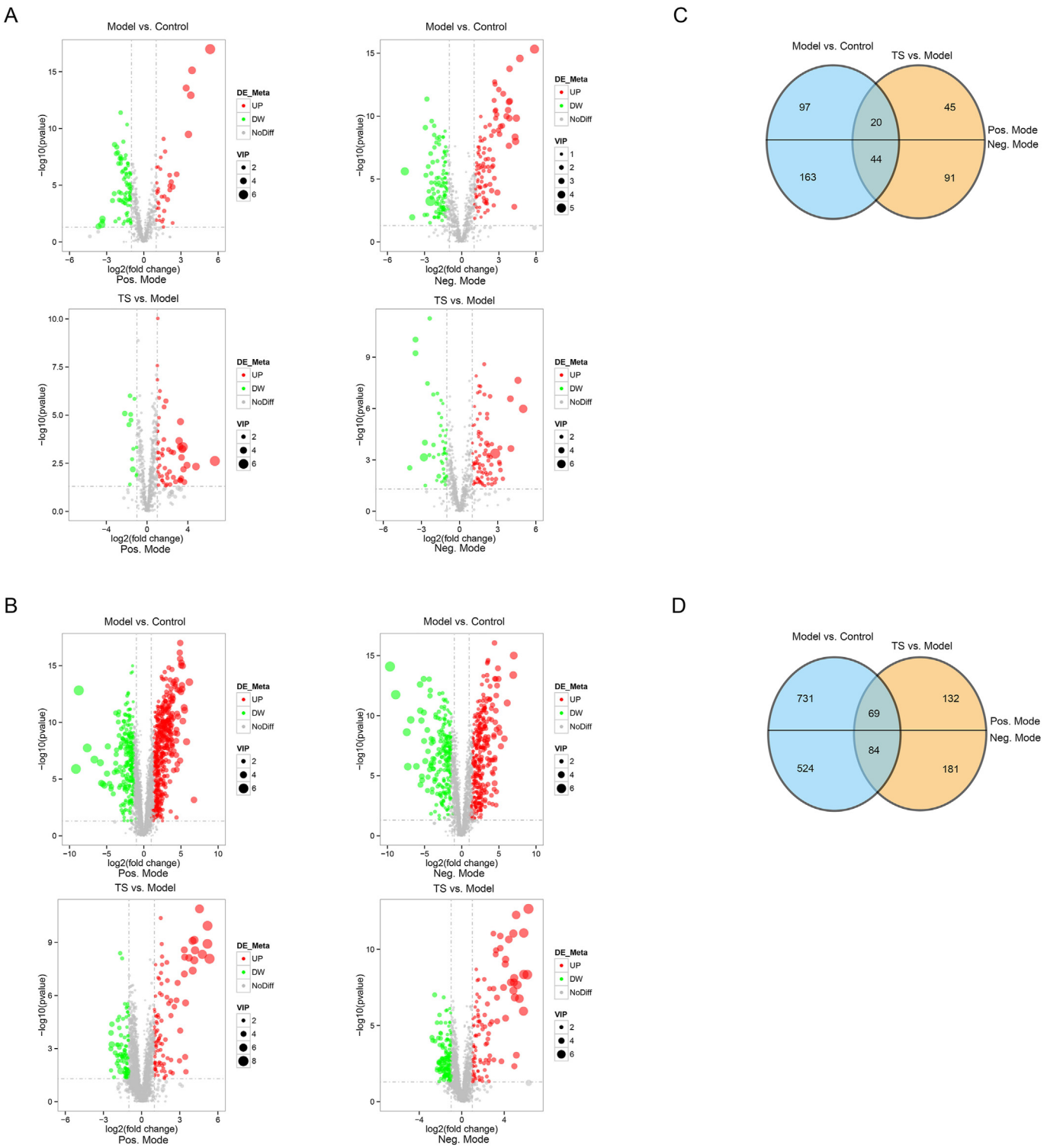

Figure 3. Volcanic plot of differential (A) serum and (B) urine metabolites with the comparison of model groups. Venn diagram of differential (C) serum and (D) urine metabolites.

p value under 0.05, in serum. Biosynthesis of unsaturated fatty acids, Metabolism of xenobiotics by cytochrome P450, Drug metabolism-cytochrome P450, Ferroptosis were significant interfered in urine ($p < 0.05$). While Purine metabolism (in serum) and Biosynthesis of unsaturated fatty acids (in urine) were the pathways with the highest concentration of metabolites (Figure 4A and B). Similarly, both of the pathways were also found interfered in Control group compared with Model group (with $p = 0.02$, $p = 0.4$ correspondingly).

Compared Control with Model group, Steroid hormone biosynthesis (in serum) and Ferroptosis (in urine) were the pathways with the highest concentration of metabolites and the most significant p value (with $p = 0.0002$, $p = 0.001$ correspondingly). Both of the pathways were also found interfered in TS group compared with Model group (with $p = 0.1$, $p = 0.2$ correspondingly). After pathway enrichment analysis of the altered metabolites, the overlap differential metabolisms of TSG group and control group were selected into Tables 1 and 2.

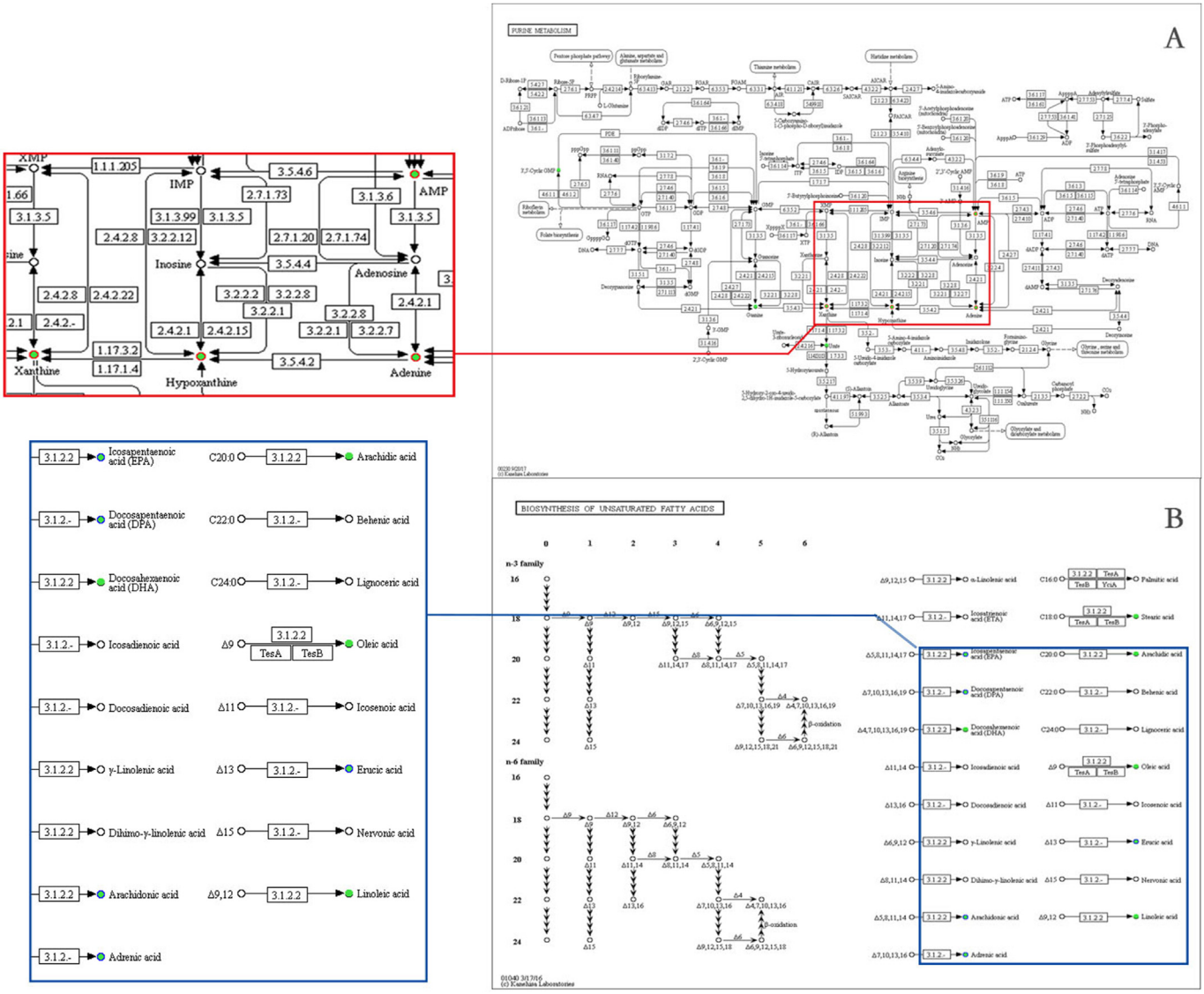

Figure 4. Pathways with most regulated metabolites annotated in serum and urine separately (A) Purine metabolism (B) Biosynthesis of unsaturated fatty acids.

3.3. Lipidomic metabolite annotated in serum and urine

4. After TSG treatment, 156 lipid metabolites in the serum (Figure 5A) and 264 in the urine (Figure 5B) were annotated to eight major category of lipids and their subcategories according to LIPIDMAPS (http://www.lipidmaps.org/). Most of them were fatty acyls. Meanwhile, there were 105 lipids annotated both in serum and urine sample, including 58 of fatty acyls, 30 of sterol lipids, 10 of prenol lipids, 4 of glycerophospholipids, and 3 of polyketides.

4. Discussion

The bioactivities of loquat leaf extract TSG were approved, including weight control, reducing TC, TG and LDL-C levels, raising HDL-C level, as well as improving glucose and insulin tolerance. According to the subsequent metabolomics studies of mice serum and urine, most of metabolites were found relevant to the function of amino acid metabolism, posteriorly lipid metabolism. Many studies showed that amino acids mediated the risk of future diabetes and were biomarkers for developing insulin resistance [20, 33]. An increase in alanine levels reflects the occurrence of insulin resistance. Some approaches can impact the synthesis of β-alanine in its metabolic pathway. This work found that β-alanine metabolism pathway was affected by up-regulation of spermidine, spermine and 4-amino-butanoate. Furthermore, previous research had investigated the role of polyamines in energy balance and glucose metabolism, indicating that spermidine supplementation improved glucose utilization in obese mice and resulted in significant weight loss [34]. The 4-amino-butanoate prevented and reversed the development of type 1 diabetes by promoting the growth and survival of β cells in mouse models, and exhibited an immunosuppressive effect, thereby protecting β cells from autoimmune damage [35]. Hence the effect of TSG on obesity and type 2 diabetes through the spermine, spermidine and 4-amino-butanoate regulation is worth to be explored in the future study.

As the second most abundant metabolites detected in serum and urine, lipidomic metabolites were annotated according to LIPIDMAPS. Most of them were fatty acyls, 58 of which were found both in serum and urine samples. Among those fatty acyl lipids, fatty acids and conjugates accounted for the majority. Fatty acids may exist as free fatty acids in mammal's body or combine with other molecules to form lipids, such as cholesterol esters, phospholipids and triglycerides [36, 37, 38, 39]. Recent research suggested that fatty acids might have an essential role in insulin resistance and T2DM. In an insulin resistant state, there was an increase in the activity of hormone sensitive lipase releasing free fatty acids into circulation [40]. On the basis, Yang et al. identified 35 potential lipid biomarkers, including 2 fatty acids, 6 triglycerides, 3

Table 1. Overlap differential metabolites of TS group and Control group in serum.

*Metabolites	Map Title	Formula	MW (Da)	RT (min)	log2FC		*p* value		VIP		Regulation	
					TS vs M	M vs C	TS vs M	M vs C	TS vs M	M vs C	TS vs M	M vs C
Hypoxanthine	Purine metabolism	$C_5H_4N_4O$	136.0384	1.515	3.516	−3.396	4.497E−04	2.926E−02	6.131	4.452	up	down
Adenine	Purine metabolism	$C_5\ H_5\ N_5$	135.0544	1.629	2.581	1.061	1.702E−02	5.150E−05	2.545	1.266	up	up
Xanthine	Caffeine metabolism	$C_5H_4N_4O_2$	152.0334	1.645	4.039	−4.000	2.168E−04	1.092E−02	4.633	3.025	up	down
Cyclohexa-1, 5-diene -1-carbonyl-CoA	Metabolic pathways	$C_{28}H_{42}N_7O_{17}P_3S$	873.1587	13.112	−1.685	1.593	3.956E−02	4.738E−02	1.580	1.430	down	up
	Steroid hormone biosynthesis											
Progesterone	Aldosterone synthesis and secretion	$C_{21}\ H_{30}\ O_2$	314.2238	13.139	−1.577	−2.008	1.820E−05	8.802E−03	2.405	1.886	down	down
Erucic acid	Biosynthesis of unsaturated fatty acids	$C_{22}H_{42}O_2$	338.3185	15.548	2.806	−2.527	4.241E−04	5.581E−04	7.485	5.678	up	down

*Overlap differential metabolites annotated by KEGG. The compounds are ordered by retention time (RT).

Table 2. Overlap differential metabolites of TS group and Control group in urine.

*Metabolites	Map Title	Formula	MW (Da)	RT (min)	log2FC		*p* value		VIP		Regulation	
					TS vs M	M vs C	TS vs M	M vs C	TS vs M	M vs C	TS vs M	M vs C
Creatine	Glycine, serine and threonine metabolism Arginine and proline metabolism	$C_4\ H_9\ N_3\ O_2$	131.0694	1.336	−1.995	1.118	6.240E−09	1.826E−04	1.401	1.308	down	up
Taurocheno-deoxycholic acid	Bile secretion Cholesterol metabolism Primary bile acid biosynthesis	$C_{26}\ H_{45}\ N\ O_6\ S$	499.29621	12.038	2.608	−1.869	5.040E−04	4.495E−03	1.870	2.298	up	down
Deoxycholic acid	Bile secretion	$C_{24}\ H_{40}\ O_4$	392.2923	12.429	3.316	−1.438	2.479E−04	1.477E−02	2.437	3.174	up	down
Arachidonic acid	Bile secretion Long-term depression Oxytocin signaling pathway Vascular smooth muscle contraction	$C_{20}\ H_{32}\ O_2$	304.2398	14.584	1.361	−1.363	1.087E−02	7.356E−03	1.025	1.706	up	down
Adrenic acid	Ferroptosis Biosynthesis of unsaturated fatty acids	$C_{22}\ H_{36}\ O_2$	332.2710	14.973	2.447	−1.938	1.855E−03	6.880E−03	1.663	2.437	up	down
Platelet-activating factor	Ether lipid metabolism Neuroactive ligand-receptor interaction	$C_{26}H_{54}NO_7P$	523.3640	15.266	2.656	−1.235	2.860E−05	1.378E−02	1.823	1.706	up	down

* Overlap differential metabolites annotated by KEGG. The compounds are ordered by retention time (RT).

cholesterol esters, 1 sphingomyelin, and 23 glycerophospholipids, closely related to the diagnosis of type 2 diabetes [41, 42].

In the subsequent pathway analysis, purine metabolism was found to be significantly interfered according to annotating differential metabolites in serum. As demonstrated in Figure 4A, xanthine, hypoxanthine, and adenine were upregulated after dosing TSG. It's worth mentioning that a significantly higher expression of adenine also existed in control groups comparing with model groups. Adenine is an activator of AMPK (AMP-activated protein kinase) [43], and activation of AMPK has been widely used in the treatment of type 2 diabetes. There is substantial evidence suggesting that AMPK is dysregulated in animals and humans with T2D, and AMPK activation (physiological or pharmacological) can improve insulin sensitivity and metabolic health [44]. In purine metabolism pathway, adenine can be synthesized by adenosine or deoxyadenosine under the action of purine-nucleoside phosphorylase, however, differential expression of the two upstream compounds was not observed in our study. We assume that it is more likely the enzyme catalyzed this reaction contributes more. Thus, it is suggested adenine plays an important role in ameliorating insulin resistance by TSG, and its synthetase purine-nucleoside phosphorylase worth to be evaluated in the future research.

Annotation of the metabolites in urine showed that, biosynthesis of unsaturated fatty acids was another pathway mainly inferenced after TSG treatment (Figure 4B). Ten compounds were assigned in the

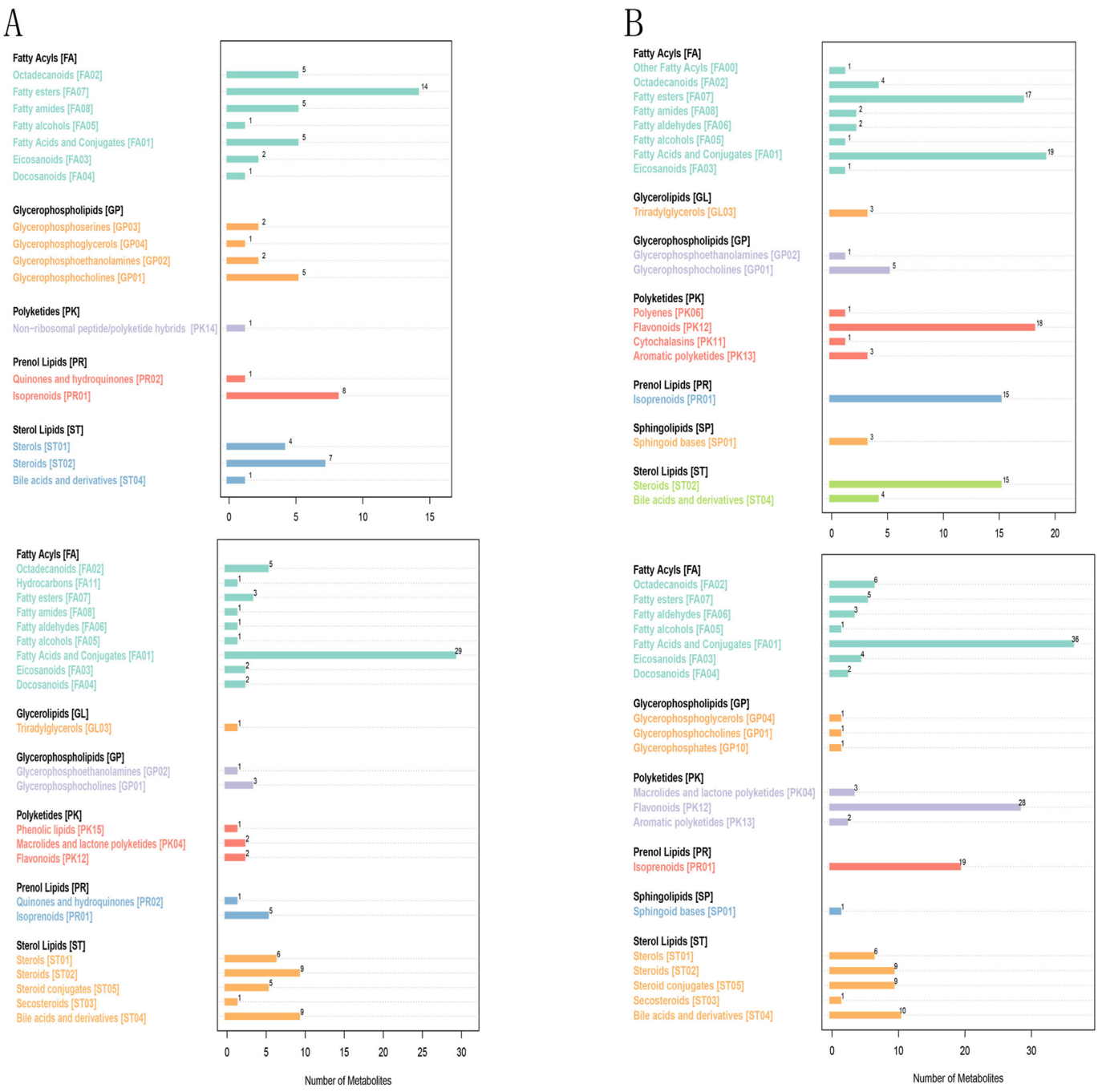

Figure 5. Function of lipid metabolites in (A) serum and (B) urine after TSG treatment detected in positive mode (the upper diagram) and negative mode (the lower diagram).

pathway with 5 of which significantly downregulated, namely eicosapentaenoic acid (EPA), docosapentaenoic acid (DPA), arachidonic acid (AA), adrenic acid (AdA), and erucic acid. EPA and DPA were approved to improve diabetes or complications, attenuating hyperglycemia and insulin resistance dramatically in db/db mice [45], attenuating the progression of albuminuria on subjects with type 2 diabetes and coronary artery disease [46]. AA and its extension product AdA are the abundant polyunsaturated fatty acids in mammalian tissues, which are usually esterified into membrane phospholipids. It was well-established that insulin secretion from pancreatic β-cells was stimulated by AA [47, 48, 49]. Further, the abnormal metabolism of AA may occur in diabetes mellitus patients with vascular disease. To the results of our research, excretion of the 5 unsaturated fatty acids were apparently reduced after dosing TSG, while the situation, 48, in serum stayed unchanged. It was inferred that TSG could improve the utilization of the 5 important unsaturated fatty acids in the process of its pharmacodynamics.

In conclusion, the diagnosis and treatment of type 2 diabetes may be closely related to the metabolic disorders of glycerophospholipids, triglycerides, cholesterol esters and sphingomyelin. Our research similarly showed that, among the lipid metabolite, fatty acyls, sterol lipids, phenol lipids, glycerophospholipids, and polyketides were impacted to varying degrees after TSG treatment. Furthermore, out of 78 annotated fatty acyls, 4 fatty acids and conjugates, 3 fatty esters, 3 octadecanoid, 1 hydrocarbon, 1 fatty amide, and 1 eicosanoid were significantly regulated. Meanwhile, 3 steroids, 2 sterols, 2 steroid conjugates, 1 of bile acids and derivatives were significantly regulated in 42 annotated sterol lipids. Therefore, fatty acyls and sterol lipids metabolism and their significant

differential metabolites deserve further investigation to reveal the mechanism of TSG treatment.

5. Conclusion

This study established that TSG from loquat leaf alleviated insulin-resistant diabetes syndrome. Untargeted metabolomics analysis of mice serum and urine found that the metabolites were apparently regulated in insulin-resistant mice, and the alteration was reversed after oral administration of TSG. The therapeutic mechanism mostly involved the regulation of purine metabolism and biosynthesis of unsaturated fatty acids. Furthermore, lipid metabolites in serum and urine were screened and analyzed, these metabolites mainly belonged to the classes of fatty acyl, sterol lipid and polyketide. The present study also provided a utilization of untargeted metabolomics followed by statistical analysis in the research of multicomponent and complex mechanism of traditional medicine.

Declarations

Author contribution statement

Ya-nan Gai: Conceived and designed the experiments; Performed the experiments; Analyzed and interpreted the data; Contributed reagents, materials, analysis tools or data; Wrote the paper.

Jiawei Li: Conceived and designed the experiments; Performed the experiments; Analyzed and interpreted the data; Contributed reagents, materials, analysis tools or data.

Tunyu Jian; Xiaoqin Ding; Han Lyu; Yan Liu; Jing Li; Bingru Ren: Performed the experiments.

Jian Chen: Conceived and designed the experiments; Contributed reagents, materials, analysis tools or data.

Weilin Li: Contributed reagents, materials, analysis tools or data.

Funding statement

This research was supported by the National Natural Science Foundation of China (No. 81773885; No. 31770366; No. 81973463) and a research grant from Jiangsu Scientific and Technological Innovations Platform (Jiangsu Provincial Service Center for Antidiabetic Drug Screening).

Data availability statement

Data included in article/supp. material/referenced in article.

Declaration of interest's statement

The authors declare no conflict of interest.

Additional information

Supplementary content related to this article has been published online at https://doi.org/10.1016/j.heliyon.2022.e11194.

References

[1] Y. Liu, W. Zhang, C. Xu, et al., Biological activities of extracts from loquat (Eriobotrya japonica Lindl.): a review, Int. J. Mol. Sci. 17 (12) (2016) 1983.
[2] H. Lv, W.L. Li, Y.P. Pei, et al., Detection of flavonoids in Eriobotrya japonica (Thunb. Lindl.) by HPLC-MS^n, Res. Pract. Chin. Med. 23 (6) (2009) 56–58.
[3] H. Lv, X. Yu, J. Chen, et al., Studies on the flavonoids from leaf of Eriobotrya japonica (Thunb.) Lindl, Chin. Tradit. Patent Med. 36 (2) (2014) 329–332.
[4] Z.L. Zhou, R. Aquino, V. Defeo, et al., Planta medica polyhydroxylated triterpenes from Eriobotrya japonica, Planta Med 56 (3) (1990) 330–332.
[5] J.H. Ju, L. Zhou, G. Lin, et al., Studies on constituents of triterpene acids from Eriobotrya japonica and their anti inflammatory and antitussive effects, Chin. Pharmaceut. J. 10 (2003) 24–29.
[6] X. Ao, L. Zhao, H. Lü, et al., New sesquiterpene glycosides from the leaves of Eriobotrya japonica, Nat. Prod. Commun. 10 (7) (2015), 1934578X1501000702.
[7] N. De Tommasi, R. Aquino, F. De Simone, et al., Plant metabolites. New sesquiterpene and ionone glycosides from Eriobotrya japonica, J. Nat. Prod. 55 (8) (1992) 1025–1032.
[8] N. De Tommasi, F. De Simone, R. Aquino, et al., Plant metabolites. New sesquiterpene glycosides from Eriobotrya japonica, J. Nat. Prod. 53 (4) (1990) 810–815.
[9] L. Zhao, J. Chen, H. Lv, et al., A new sesquiterpene glycoside from the leaves of Eriobotrya japonica, Chem. Nat. Compd. 51 (6) (2015) 1103–1106.
[10] L. Zhao, J. Chen, M. Yin, et al., Analysis of sesquiterpene glycosides from loquat leaves by UPLC-Q-TOF-MS, Chin. Tradit. Patent Med. 37 (7) (2015) 1498–1502.
[11] R. Yanagisawa, Y. Oshima, Y. Okada, et al., A sesquiterpene glycoside, Loquatifolin A, from the leaves of Eriobotrya japonica, Chem. Pharm. Bull. 36 (4) (1988) 1270–1274.
[12] J. Chen, W.L. Li, J.L. Wu, et al., Hypoglycemic effects of a sesquiterpene glycoside isolated from leaves of loquat (Eriobotrya japonica (Thunb.) Lindl.), Phytomedicine 15 (1) (2008) 98–102.
[13] N. De Tommasi, F. De Simone, G. Cirino, et al., Hypoglycemic effects of sesquiterpene glycosides and polyhydroxylated triterpenoids of Eriobotrya japonica, Planta Med. 57 (5) (1991) 414–416.
[14] T. Jian, X. Ao, Y. Wu, et al., Total sesquiterpene glycosides from Loquat (Eriobotrya japonica) leaf alleviate high-fat diet induced non-alcoholic fatty liver disease through cytochrome P450 2E1 inhibition, Biomed. Pharmacother. 91 (2017) 229–237.
[15] T. Jian, Y. Wu, X. Ding, et al., A novel sesquiterpene glycoside from Loquat leaf alleviates oleic acid-induced steatosis and oxidative stress in HepG2 cells, Biomed, Pharmacother. 97 (2018) 1125–1130.
[16] J. Li, X. Ding, T. Jian, et al., Four sesquiterpene glycosides from loquat (Eriobotrya japonica) leaf ameliorates palmitic acid-induced insulin resistance and lipid accumulation in HepG2 Cells via AMPK signaling pathway, PeerJ 8 (2020), e10413.
[17] P. Richard, P. Shin, T. Beeson, et al., Quality and cost of diabetes mellitus Care in community health centers in the United States, PLoS One 10 (12) (2015), e0144075.
[18] P. Zimmet, K.G. Alberti, J. Shaw, Global and societal implications of the diabetes epidemic, Nature 414 (6865) (2001) 782–787.
[19] (a) R. Lipi, F. Dotta, L. Marselli, et al., Prolonged exposure to free fatty acid has cytostatic and pro-apoptotic effects on human pancreatic islets, Diabetes 51 (2002) 1437–1443;
(b) S.M. Honoré, M.V. Grande, J. Gomez Rojas, et al., Smallanthus sonchifolius (Yacon) flour improves visceral adiposity and metabolic parameters in high-fat-diet-fed rats, J. Obes. (2018), 5341384–5341384.
[20] (a) R.H. Unger, Y.T. Zhou, Lipotoxicity of beta-cells in obesity and other causes of fatty acid spilover, Diabetes 50 (Suppl 1) (2001) S1l8–S121;
(b) S. Cinti, G. Mitchell, G. Barbatelli, et al., Adipocyte death defines macrophage localization and function in adipose tissue of obese mice and humans, J. Lipid Res. 46 (11) (2005) 2347–2355.
[21] J.M. Moreno-Navarrete, J.M. Fernández-Real, The complement system is dysfunctional in metabolic disease: evidences in plasma and adipose tissue from obese and insulin resistant subjects, Semin. Cell Dev. Biol. 85 (2019) 164–172.
[22] P. Petrus, F. Rosqvist, D. Edholm, et al., Saturated fatty acids in human visceral adipose tissue are associated with increased 11-beta-hydroxysteroid-dehydrogenase type 1 expression, Lipids Health Dis. 14 (2015) 42.
[23] X. Wang, H. Sun, A. Zhang, et al., Wang, Potential role of metabolomics apporoaches in the area of traditional Chinese medicine: as pillars of the bridge between Chinese and Western medicine, J. Pharm. Biomed. Anal. 55 (5) (2011) 859–868.
[24] A. Zhang, H. Sun, Z. Wang, et al., Metabolomics: towards understanding traditional Chinese medicine, Planta Med. 76 (17) (2010) 2026–2035.
[25] G. Tang, S. Li, C. Zhang, et al., Clinical efficacies, underlying mechanisms and molecular targets of Chinese medicines for diabetic nephropathy treatment and management, Acta Pharm. Sin. B 11 (9) (2021) 2749–2767.
[26] Y. He, H. Zhang, Y. Yang, et al., Using metabolomics in diabetes management with traditional Chinese medicine: a review, Am. J. Chin. Med. 49 (8) (2021) 1813–1837.
[27] Y. Chen, Y.M. Tang, S.L. Yu, et al., Advances in the pharmacological activities and mechanisms of diosgenin, Chin. J. Nat. Med. 13 (8) (2015) 578–587.
[28] B. Pang, L.H. Zhao, Q. Zhou, et al., Application of berberine on treating type 2 diabetes mellitus, Internet J. Endocrinol. 2015 (2015), 905749.
[29] Q. Nie, H. Chen, J. Hu, et al., Dietary compounds and traditional Chinese medicine ameliorate type 2 diabetes by modulating gut microbiota, Crit. Rev. Food Sci. Nutr. 59 (6) (2019) 848–863.
[30] L. Pan, Z. Li, Y. Wang, et al., Network pharmacology and metabolomics study on the intervention of traditional Chinese medicine Huanglian Decoction in rats with type 2 diabetes mellitus, J. Ethnopharmacol. 258 (2020), 112842.
[31] Y. He, H. Zhang, Y. Yang, et al., Using metabolomics in diabetes management with traditional Chinese medicine: a review, Am. J. Chin. Med. 49 (8) (2021) 1813–1837.
[32] T. Jian, C. Yu, X. Ding, et al., Hepatoprotective effect of seed coat ofEuryale ferox extract in non-alcoholic fatty liver disease induced by high-fat diet in mice by increasing IRs-1 and inhibiting CYP2E1, J. Oleo Sci. 68 (6) (2019) 581–589.
[33] J.C. Floyd Jr., S.S. Fajans, J.W. Conn, et al., Stimulation of insulin secretion by amino acids, J. Clin. Investig. 45 (9) (1966) 1487–1502.
[34] S.K. Sadasivan, B. Vasamsetti, J. Singh, et al., Exogenous administration of spermine improves glucose utilization and decreases bodyweight in mice, Eur. J. Pharmacol. 729 (2014) 94–99.

[35] C. Ruocco, M. Ragni, F. Rossi, et al., Manipulation of dietary amino acids prevents an reverses obesity in mice through multiple mechanisms that modulate energy homeostasis, Diabetes 69 (11) (2020) 2324.
[36] G.J. Betts, P. Desaix, E. Johnson, et al., Human Anatomy and Physiology, OpenStax College, 2013.
[37] P.V. Röder, B. Wu, Y. Liu, et al., Pancreatic regulation of glucose homeostasis, Exp. Mol. Med. 48 (2016) e219.
[38] V.L. Tokarz, P.E. MacDonald, A. Klip, The cell biology of systemic insulin function, J. Cell Biol. 217 (2018) 2273–2289.
[39] V.T. Samuel, G.I. Shulman, Mechanisms for insulin resistance: common threads and missing links, Cell 148 (2012) 852–871.
[40] S.S. Shetty, Fatty acids and their role in type-2 diabetes (Review), Exp. Ther. Med. 22 (2021) 706.
[41] W. Yang, Y. Chen, C. Xi, et al., Liquid chromatography–Tandem mass spectrometry-based plasma metabonomics delineate the effect of metabolites' stability on reliability of potential biomarkers, Anal. Chem. 85 (5) (2013) 2606–2610.
[42] C. Xi, Y.H. Chen, W. Yang, et al., Development of method for serum preparation and lipidomics analysis based on rapid resolution liquid chromatography-mass spectrometry, Chin. J. Anal. Chem. 41 (9) (2013) 1308–1314.
[43] J.G. Leu, M.H. Chiang, C.Y. Chen, et al., Adenine accelerated the diabetic wound healing by PPAR delta and angiogenic regulation, Eur. J. Pharmacol. 818 (2018) 569–577.
[44] K.A. Coughlan, R.J. Valentine, N.B. Ruderman, et al., AMPK activation: a therapeutic target for type 2 diabetes? Diabetes Metab. Syndr. Obes. 7 (2014) 241–253.
[45] P. Zhuang, H. Li, W. Jia, et al., Eicosapentaenoic and docosahexaenoic acids attenuate hyperglycemia through the microbiome-gut-organs axis in db/db mice, Microbiome 9 (1) (2021) 185.
[46] T.K. Elajami, A. Alfaddagh, D. Lakshminarayan, et al., Eicosapentaenoic and docosahexaenoic acids attenuate progression of albuminuria in patients with type 2 diabetes mellitus and coronary artery disease, J. Am. Heart Assoc. 6 (7) (2017), e004740.
[47] B.A. Wolf, S.M. Pasquale, J. Turk, Free fatty acid accumulation in secretagogue-stimulated pancreatic islets and effects of arachidonate on depolarization-induced insulin secretion, Biochemistry 30 (26) (1991) 6372–6379.
[48] A.M. Band, P.M. Jones, S.L. Howell, Arachidonic acid-induced insulin secretion from rat islets of Langerhans, J. Mol. Endocrinol. 8 (2) (1992) 95–101.
[49] P.M. Jones, S.J. Persaud, Arachidonic acid as a second messenger in glucose-induced insulin secretion from pancreatic β-cells, J. Endocrinol. 137 (1) (1993) 7–14.